Evidence for kinetic Alfvén waves and parallel electron energization at 4–6 R_E altitudes in the plasma sheet boundary layer

J. R. Wygant,[1] A. Keiling,[1] C. A. Cattell,[1] R. L. Lysak,[1] M. Temerin,[2] F. S. Mozer,[2] C. A. Kletzing,[3] J. D. Scudder,[3] V. Streltsov,[4] W. Lotko,[4] and C. T. Russell[5]

Received 15 May 2000; accepted 26 July 2001; published 24 August 2002.

[1] We present evidence based on measurements from the Polar spacecraft for the existence of small-scale, large-amplitude kinetic Alfvén waves/spikes at the plasma sheet boundary layer (PSBL) at altitudes of 4–6 R_E. These structures coincide with larger-scale Alfvénic waves that carry a large net Poynting flux along magnetic field lines toward the Earth. Both structures are typically observed in the PSBL but have also been observed deeper in the plasma sheet. The small-scale spikes have electric field amplitudes up to 300 mV m^{-1} and associated magnetic field variations between 0.5 and 5 nT. Previous analysis has shown that the larger-scale Alfvén waves have periods of ~20–60 s and carry enough Poynting flux to explain the generation of the most intense auroral structures observed in the Polar Ultraviolet Imager data set. In this paper it is shown that the smaller-scale waves have durations in the spacecraft frame of 250 ms to 1 s (but may have shorter time durations since the Nyquist frequency of the magnetic field experiment is ~4 Hz.). The characteristic ratio of the amplitudes of the electric to magnetic field fluctuations is strong evidence that the waves are kinetic Alfvén waves with scale sizes perpendicular to the magnetic field on the order of 20–120 km (with an electron inertial length c/ω_{pe}~10 km and an ion gyroradius ~20 km). Theoretical analysis of the observed spikes suggests that these waves should be very efficient at accelerating electrons parallel to the magnetic field. Simultaneously measured electron velocity space distribution functions from the Polar Hydra instrument include parallel electron heating features and earthward electron beams, indicating strong parallel energization. The characteristic parallel energy is on the order of ~1 keV, consistent with estimates of the parallel $\int Edl$ associated with small-scale kinetic Alfvén wave structures. The energy flux in the electron "beams" is ~0.7 ergs cm^{-2} s^{-1}. These observations suggest that the small-scale kinetic Alfvén waves are generated from the larger-scale Alfvén waves through one or more of a variety of mechanisms that have been proposed to result in the filamentation of large-amplitude Alfvén waves. The observations presented herein provide strong evidence that in addition to the auroral particle energization processes known to occur at altitudes between 0.5 and 2 R_E, there are important heating and acceleration mechanisms operating at these higher altitudes in the plasma sheet. *INDEX TERMS:* 2712 Magnetospheric Physics: Electric fields (2411); 2748 Magnetospheric Physics: Magnetotail boundary layers; 2752 Magnetospheric Physics: MHD waves and instabilities; 2704 Magnetospheric Physics: Auroral phenomena (2407)

1. Introduction

[2] One of the outstanding problems in magnetospheric physics is the nature of the energy transfer processes that carry energy from the reconnection region in the geomagnetic tail to where it is ultimately deposited in the ionosphere of the Earth. During a typical magnetospheric substorm a large portion of the energy extracted from the solar wind that remains in the Earth's magnetosphere is ultimately deposited in the terrestrial ionosphere by intense beams of electrons with energy fluxes ranging between 1 and 100 ergs cm^{-2} s^{-1} at 100-km altitude and which create the aurora. A large fraction of this extremely efficient

[1]School of Physics and Astronomy, University of Minnesota, Minneapolis, Minnesota, USA.
[2]Space Sciences Laboratory, University of California, Berkeley, California, USA.
[3]Department of Physics and Astronomy, University of Iowa, Iowa City, Iowa, USA.
[4]Thayer School of Engineering, Dartmouth College, Hanover, New Hampshire, USA.
[5]Institute of Geophysics and Planetary Physics, University of California, Los Angeles, California, USA.

0148-0227/02/2001JA900113$09.00

collisionless electron energization process occurs in the auroral acceleration region at altitudes between 1000 km and 3.5 R_E [*Mozer and Hull*, 2001; *Reiff*, 1993; *Mozer et al.*, 1980].

[3] In this paper, using data from the Polar spacecraft, we address the physical processes that occur above the auroral acceleration region at altitudes of 4–7 R_E in the plasma sheet. We provide the first evidence for small-scale kinetic Alfvén waves in the plasma sheet and plasma sheet boundary layer (PSBL), which may play an important role in the local heating of the plasma sheet and also may produce earthward, magnetic field-aligned electron beams and transversely heated ions. The data suggest that the waves may result from the striation or filamentation of the large-scale Alfvén waves and that these processes may be a significant energy drain on large-scale Alfvén waves propagating through these regions of space.

[4] Historically, the PSBL has been regarded as a region of strong energy transfer between the distant tail and the auroral ionosphere [*Eastman et al.*, 1984; *Fairfield*, 1987]. However, it is only recently, with the availability of the necessary measurements from the Polar spacecraft, that a relatively complete inventory of the important energy transfer mechanisms along plasma sheet magnetic field lines above the bulk of the auroral acceleration region has become possible. Recent observations [*Wygant et al.*, 2000] (hereinafter referred to as W1) at altitudes of 4–6 R_E in the PSBL and deeper within the plasma sheet show that large amounts of energy are transferred earthward by the Poynting flux carried by Alfvén waves. This enhanced Alfvénic Poynting flux dominates other forms of energy flux along plasma sheet magnetic field lines and coincides with magnetically conjugate intense aurora. The Alfvénic Poynting flux coincided with a nearly equal ($\times$ 1/2) enhancement in the net local electron kinetic energy flux toward the Earth. The in situ ion kinetic energy flux was also ~1–2 orders of magnitude less. The Poynting flux due to the steady state magnetic field perturbations associated with the field-aligned currents and the convection electric field was estimated to be ~1–2 orders less than the Alfvénic Poynting flux. (Plots of these comparisons were not explicitly shown by W1 but are shown here.) Polar observations by W1 provide evidence that the Alfvénic Poynting flux is responsible for transferring the power needed for the acceleration of all the energized auroral particle populations accelerated into the ionosphere and also streaming out into the magnetosphere, as well as the Joule heating of the ionosphere. This makes the transmission of intense Alfvén Poynting flux along plasma sheet magnetic field lines a crucial link in magnetospheric dynamics. It provides constraints on the nature of the energy conversion processes in the distant tail and on the nature of collisionless auroral acceleration processes at lower altitudes. It also provides a source of free energy for driving particle acceleration and heating all along plasma sheet magnetic field lines.

[5] We examine in detail high time resolution electric and magnetic field data during a plasma sheet crossing obtained on 9 May 1997, which is one of the events discussed by W1. This event was among the upper 3% of the most intense electric field events observed during 400 orbits surveyed during 1997 [*Keiling et al.*, 2001]. The work by Keiling et al. (Figure 12 in that paper) indicates that the 9 May 1997 PSBL crossing and its associated large electric fields and Poynting flux, along with other similar events, occur over periods of 1–3 min during the onset time and expansion phase of substorms as determined from the profile of H bays at magnetically conjugate stations. A similar analysis by *Toivanen et al.* [2001] for two PSBL crossings showed that the period of strong earthward Poynting flux coincided within 1 min of the onset of H bays near the foot of the Polar magnetic field line.

[6] In this paper we focus on the small-scale structure of electric and magnetic fields on plasma sheet magnetic field lines, its relation to the larger-scale Alfvén waves, and evidence that the small-scale waves can efficiently heat and accelerate particles. The observations from the 9 May 1997 event show that the large-scale Alfvén waves can striate into intense, small temporal/spatial scale electric field spikes. This paper provides the first evidence, on the basis of the ratio of electric to magnetic fields, that these small-scale spikes are kinetic Alfvén waves with spatial scale sizes of ~20 km perpendicular to the magnetic field. This spatial scale is close to both the electron inertial scale and the ion acoustic gyroradius. In this paper we adopt the nomenclature discussed by *Lysak and Lotko* [1996] and used by many other studies. In that paper, small-scale Alfvén waves, which include either effects due to small perpendicular scale sizes of the order of the electron inertial scales (c/ω_{pe}) or kinetic effects associated with electron pressure and ion acoustic gyroradius, effects are called "kinetic Alfvén waves." Generally, the inertial limit of kinetic Alfvén waves is appropriate for plasma parameters at altitudes below ~5 R_E, while the kinetic limit of kinetic Alfvén waves [*Hasegawa*, 1976] is appropriate for altitudes above ~5 R_E in the hot plasma sheet. It should be noted that our observations take place in the transition region where both effects are important. Another significant feature of this region is that the electron thermal velocity is roughly comparable to the Alfvén velocity, leading to the possibility of resonate interactions between waves and electrons. Kinetic Alfvén waves with perpendicular scales on the order of an electron inertial length are of particular interest because they are often associated with small but significant parallel electric fields extending over a very long distance parallel to B and can efficiently accelerate charged particles through this electric field. Electron distribution functions from the Hydra instrument are presented, providing strong circumstantial evidence that parallel acceleration is occurring.

[7] Although our interest has focused on the PSBL, we stress that events with large Alfvénic Poynting flux toward the Earth also occur deeper in the plasma sheet. Since the Polar spacecraft spends less time in the PSBL (1–3 min) compared to the rest of the plasma sheet (30–50 min), the statistics of these events suggest that the most intense Alfvénic electric fields may have a higher frequency of occurrence in the PSBL. A study by C. A. Kletzing et al. (unpublished manuscript, 1999) of the occurrence of intense electric fields as a function of position relative to the outer boundary and inner edge of the plasma sheet indicates that the most intense events have a stronger probability of occurring near the outer boundary of the plasma sheet, while less intense events are more uniformly distributed. The first observations of intense Poynting flux in associa-

tion with Alfvén waves was by *Maynard et al.* [1996] using CRRES data obtained during a substorm-related particle injection event near the inner edge of the plasma sheet. The peak value of the Poynting flux during this CRRES event was ~0.8 ergs cm^{-2} s^{-1} and directed earthward along the magnetic field. Thus it is clear that Alfvénic Poynting flux is an important energy transfer mechanism throughout the plasma sheet.

[8] Observations from the electric field instrument on the ISEE 1 spacecraft have shown that intense, small-scale electric field structures with amplitudes of > 100 mV m^{-1} on timescales comparable to the instrument sampling resolution of one tenth of a second are often present on plasma sheet field lines in the tail ranging out to the spacecraft apogee at 22 R_E [*Cattell et al.*, 1982]. *Streed et al.* [2002] have shown that such fields occur out to a radial distance of 100 R_E. Since the ISEE electric field booms only measured the electric field component in the spin plane of the spacecraft (which coincided with the ecliptic plane), ISEE 1 provided no information on the nature of the electric fields normal to the plasma sheet boundary near ISEE apogee. This is the dominant component of the electric field at the PSBL at Polar altitudes. The ratio of E/B could not be unambiguously determined in the ISEE data set, owing to differences between the sampling rates and signal filtering of the electric and magnetic field instruments.

[9] At lower altitudes, observations of intense, small perpendicular-scale electric fields by the S3–3 [*Mozer et al.*, 1980], Viking [*Block and Falthammer*, 1990], DE 1 [*Weimer and Gurnett*, 1993], Freja [*Louarn, et al.*, 1994], Fast Auroral Snapshot (FAST) [*Carlson et al.*, 1998; *Ergun et al.*, 1998], the Polar spacecraft [*Mozer et al.*, 1997] and sounding rockets have been interpreted in terms of kinetic Alfvén waves, Alfvén waves, and/or electrostatic shocks. The finite parallel electric field component associated with kinetic Alfvén waves has been invoked as one of the means of accelerating electron beams in the auroral acceleration region [*Goertz*, 1984; *Lysak and Lotko*, 1996; *Lysak*, 1998; *Streltsov and Lotko*, 1995; *Temerin et al.*, 1986; *Hui and Seyler*, 1992; *Kletzing*, 1994], while the strong perpendicular components have been used to explain the transverse acceleration of ions to produce conical distributions [*Temerin and Roth*, 1986].

[10] The electric field measurements presented herein are obtained from the University of California, Berkeley, electric field instrument [*Harvey et al.*, 1995] on the Polar spacecraft. The electric field is determined through measurement of the electric potential difference between pairs of current-biased spherical sensors. These sensors are deployed at the ends of three orthogonal pairs of booms with tip-to-tip separations of 100 and 160 m in the spin plane and 13.8 m along the spin axis. The three-dimensional electric field vector is sampled at 20 samples s^{-1} during the event presented here.

[11] The electric field and Poynting flux values for the 9 May 1997 event presented in this paper are a factor of 1.3 larger than the values presented by W1. This is because in the previous paper, the analysis programs did not include a standard constant factor associated with the effective antenna length of conducting booms in a plasma for which the Debye length is much larger than the boom length. This factor was first predicted in the original proposal for the ISEE 1 spherical double-probe electric field experiment (F. S. Mozer, personal communication, 2000). It was subsequently verified by extensive comparison in the solar wind of the electric field measured by the spherical double-probe instrument to that derived from $\mathbf{E}=-\mathbf{v}\times\mathbf{B}$, where $\mathbf{v}$ is the measured plasma flow velocity and $\mathbf{B}$ is the measured magnetic field [*Pedersen et al.*, 1985]. No conclusions of W1 are modified by this change.

[12] The magnetic field vector is sampled at 8.3 samples s^{-1} by the University of California, Los Angeles (UCLA), three-dimensional fluxgate magnetometer [*Russell et al.*, 1995]. The fluxgate data are filtered at 4 Hz to avoid aliasing. The Hydra particle detector on Polar [*Scudder et al.*, 1995] provides measurements of electron and ion density, temperature, energy flux, and two-dimensional velocity space distribution with a 13.8-s time resolution.

2. Large-Scale Structure of the Tail Lobe – Plasma Sheet Boundary

[13] Figure 1, derived from W1 (and discussed in more detail there), provides the large-scale context for the small-scale structures and distribution functions to be discussed in section 3. Figure 1 presents 45 min of data beginning at 0530 UT on 9 May 1997 during a passage of the Polar spacecraft from the tail lobe into the plasma sheet. Figure 1a presents the x component of the electric field, which is directed normal to the ecliptic plane in a northward direction. In this event it is nearly perpendicular to the ambient magnetic field. Figure 1b presents the y component of the magnetic field, which is directed perpendicular to the magnetic field and x direction. A model magnetic field [*Tsyganenko*, 1989] has been subtracted from the magnetic field measurements to obtain this component. Figure 1c displays the magnetic field–aligned component of the wave Poynting flux derived from the detrended vector electric and magnetic fields. Positive is toward the Earth in the Northern Hemisphere. The scale on the left-hand side of Figure 1c corresponds to the value of the in situ Poynting flux. The scale on the right-hand side corresponds to the value of the Poynting flux if it is mapped along converging magnetic field lines to altitudes of 100 km, assuming no power dissipation. Figure 1d presents the electron and ion kinetic energy flux derived from the Hydra particle measurements. Figure 1e presents the electron density. Figures 1f–1h present the color-coded electron differential energy flux. The three panels consist of the differential energy flux binned into pitch angles along the magnetic field and toward the Earth (0–30°), 90° to the magnetic field (75–105°), and away from the Earth (anti-parallel to the magnetic field between 150 and 180°). Figures 1i–1k consist of the ions in the same format. The boundary between the low-density tail lobes and the plasma sheet, which is indicated by the electron density jump and the sharp increase in particle fluxes at all pitch angles, is encountered at ~0537 UT. As discussed by W1, the dominant electric and magnetic field signatures are associated with a very large amplitude Alfvén wave with a large net Poynting flux (>1 erg cm^{-2} s^{-1}) propagating toward the Earth. The Poynting flux mapped to 100-km altitude exceeds 100 ergs cm^{-2} s^{-1}. The principal conclusions of W1 were that during the period of this strong Poynting flux, the magnetic field line passing through the Polar spacecraft

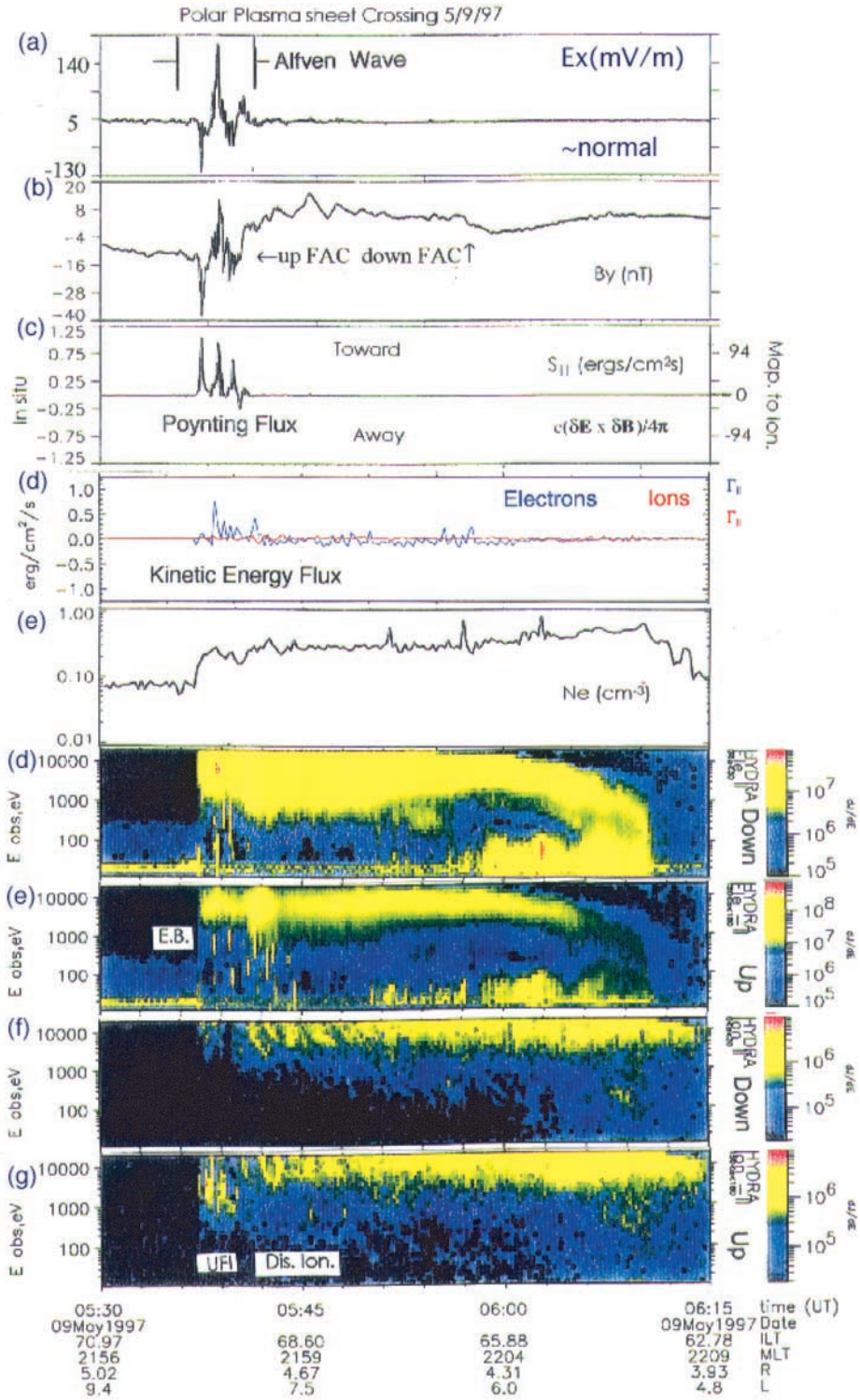

Figure 1. Polar measurements through the plasma sheet tail lobe boundary. (a) *Ex* component of the electric field (northward, normal to average plasma sheet boundary and nearly perpendicular to the magnetic field). (b) *By* component of magnetic field (eastward perpendicular to the magnetic field nominally in the plane of the plasma sheet). (c) Field-aligned component of the Poynting flux (positive is earthward). (d) Electron (blue line) and ion (red line) kinetic energy flux derived from the Hydra particle measurements. (e) Electron density. (f–k) Ion and electron fluxes for pitch angles between 150 and 180° (away from the Earth), 75 and 105 °, and 0 and 30° (toward the Earth).

was magnetically conjugate to an intense auroral structure and that the peak Poynting flux when mapped to 100 km along converging magnetic field lines, was several times that necessary to power the auroral acceleration process. Other evidence for the close relation between this Alfvén wave structure and auroral acceleration processes includes the observations at 0537 UT of magnetic field-aligned ion fluxes flowing away from the Earth over the energy range from 1 to 10 keV, as shown in Figure 1k. These upward flowing ions could be beams accelerated parallel to the magnetic field by a parallel electric field. Alternatively, observed ion distributions could be ion conics that have been heated transverse to the magnetic field by low-altitude wave fields and then ejected away from the Earth by the magnetic mirror force. In the second possibility, the ions at the higher altitudes of the Polar spacecraft would be more aligned along the magnetic field (and beam like), owing to the magnetic mirror force. Since the accelerated ions that result from both mechanisms are strongly field-aligned, it is difficult to distinguish between the two. Measurements of two-dimensional (2-D) distribution functions provided in Figure 6 provide evidence for both populations. In Figure 1f there are also brief intervals of strong electron fluxes directed toward the Earth between 0537 and 0541 UT and coincident with the period of strong Poynting flux. These appear as short, yellow vertical strips in the first colored electron differential energy flux panel, which corresponds to pitch angles of 0–30°. The behavior of the electrons streaming away from the Northern Hemisphere ionosphere (Figure 1h) is somewhat different. These fluxes are also intense and intermittent, and they also begin with entry into the plasma sheet but persist for a much longer period of time and deeper into the plasma sheet than the Alfvénic Poynting flux. Thus there is strong evidence that the magnetic field lines with strong earthward Alfvénic Poynting flux are associated with intervals of strong upward flowing ions (UFIs) and downward electron fluxes, but there is no clear relation with upward flowing electrons.

[14] The full electric field vector in magnetic-field-aligned coordinates has been presented previously by W1. The component of the electric field parallel to B is quite small compared to the several hundred mV m^{-1} perpendicular component and is in fact consistent with this field being less than several mV m^{-1}. This small parallel component could be the result of uncertainties of $\sim$ 1 degree in the instantaneous magnetic field direction and therefore may not be real.

[15] Since the large temporal/spatial scale Alfvén wave has a period in the spacecraft frame of $\sim$10–20 s, which is much larger than the periods of the shorter-duration structures that we will present in Figure 3, we will call this wave the ''large-scale'' Alfvén wave. The electric field associated with the large-scale Alfvén wave ranges up to $\sim$300 mV m^{-1} (peak-to-peak, ptp), and the magnetic field variations are on the order of 40 nT (ptp). The electric field is predominantly in the direction normal to the ecliptic, which is approximately along the normal to the plasma sheet boundary. The perturbation magnetic field is predominantly in the plane of the plasma sheet and transverse to the average magnetic field direction. For the large-scale Alfvén wave the ratio of E to B is $\sim$ 8 mV m^{-1} nT^{-1} or consistent with a phase velocity of $\sim$8000 km s^{-1}. This is roughly consistent with the value of the Alfvén velocity of $\sim$12,000 km s^{-1} (assuming 100% H^+) estimated from the measured magnetic field magnitude of 400 nT and a density of $\sim$0.4 cm^{-3}. The assumption that H^+dominates over $O^+$is supported by the inspection of ion composition measurements by the Toroidal Imaging Mass Angle Spectrometer (TIMAS) instrument during this event (W. Peterson, personal communication, 2000). This ratio, as discussed by W1, is much larger than that expected for steady state closure through typical ionospheric conductivities. The simplest explanation for this ratio of E to B is that the waves are Alfvén waves.

[16] In Figure 2 the magnetic field-aligned component of the Poynting flux associated with Alfvénic fluctuations is explicitly compared (for the first time in the literature) to the large-scale Poynting flux estimated from the magnetic perturbation associated with the large-scale field-aligned current system and the large-scale convection electric field. The Poynting flux for each panel in Figure 2 is calculated as the product of Ex and By. We rely on these two components because the x component of the electric field that lies in the spin plane of the spacecraft is measured by the long 50- and 65-m booms, and the measurement of this component of the electric field is especially accurate, an important consideration when measuring the $\sim$1 mV m^{-1} large-scale convection electric field. The validity of this approach is aided by the fact that the dominant component of the field-aligned current magnetic field perturbation is in the y direction (cross tail). The magnetic field perturbations associated with upward (Region 1) and downward current systems are shown in Figure 1b and denoted by ''FAC.'' The contribution to the Poynting flux from the large-scale field-aligned current (FAC) system and convection electric field is calculated using data that have not been detrended but that have been averaged over 6 min. In contrast, in order to calculate the contribution to the Poynting flux due to the Alfvénic fluctuations shown in Figure 1, the electric field and magnetic field data have been detrended over 180 s. Notice that the large-scale Poynting flux over this time interval is nearly undetectable on this scale and is limited to less than 0.04 ergs cm^{-2} s^{-1}. The dominance of the peak value of the Alfvénic Poynting flux over that due to the global FAC system and the convection electric field may be understood from an inspection of Figure 1. Figure 1 shows the magnetic field perturbations due to steady state field-aligned currents that are comparable to those of the Alfvén wave, but the electric field of the Alfvén wave is almost 2 orders of magnitude larger than the <4 mV m^{-1} large-scale convection electric field. If mapped to 100-km altitude along converging magnetic field lines, the Poynting flux due to the large-scale electric fields and FAC system is $\sim$4 ergs cm^{-2} s^{-1}, while, as discussed in section 2, the Alfvénic Poynting flux exceeds 100 ergs cm^{-2} s^{-1}.

3. Small-Scale Structure of the Tail Lobe–Plasma Sheet Boundary

[17] Figure 3 presents an expanded view of the electric and magnetic fields during the 25-min subinterval coinciding with the Alfvén waves and the outer boundary of the plasma sheet. The data are presented in a magnetic field-aligned coordinate system in which the x component is perpendicular to the magnetic field and is directed nearly normal to the average plasma sheet boundary (very similar to the z component of Figure 1). The y component is

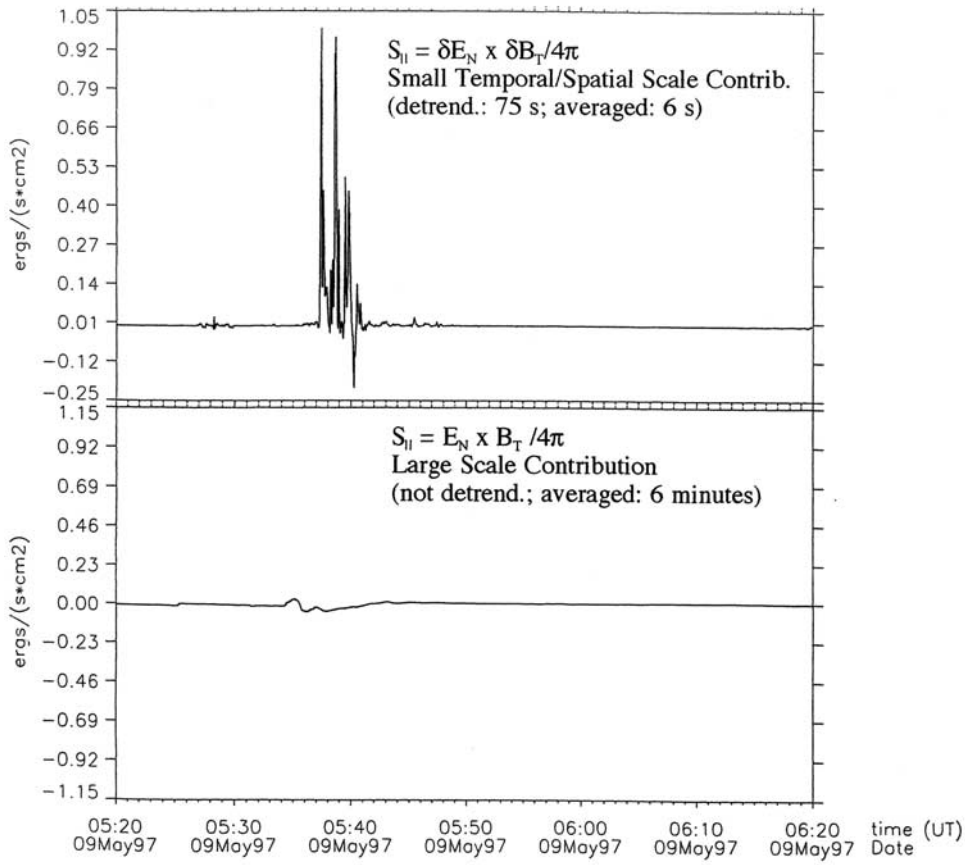

Figure 2. Comparison of estimates of (top) the Poynting flux due to the Alfvénic fluctuations and (bottom) the Poynting flux due to global field-aligned currents and the large-scale convection electric field for the plasma sheet boundary layer (PSBL) crossing on 9 May 1997.

directed perpendicular to the magnetic field in a nearly azimuthal direction. Figure 3a shows the x component of the electric field data at the full resolution of 20 samples s^{-1}. Figure 3b shows the y component of the magnetic field at the full resolution of ~9 samples s^{-1}. Figures 3c and 3d show the electric and magnetic field data after they have been averaged to produce a time resolution with a Nyquist frequency of 4 Hz. These data have also been detrended to remove variations slower than the spin period of 6 s. Figure 3d shows the Poynting flux calculated from the electric and magnetic fields over the frequency range from 0.17 to 4 Hz. Figures 3a and 3c show that embedded in the large-scale Alfvén wave are individual electric field spikes with amplitudes to ~400 mV m^{-1} (ptp). The effect of the filtering in Figures 3c and 3d is to show a general correlation between the electric field and magnetic field pulses on this timescale. The magnetic field fluctuations are on the order of ~1–10 nT (ptp). The ratio of the amplitudes of the electric to the magnetic field fluctuations equal 20–50 mV $(m \cdot nT)^{-1}$ and yields a ratio for the higher-frequency waves a factor of 2–5 greater than that expected for an Alfvén wave but consistent with kinetic Alfvén waves. As shown in section 4, a comparison of the ratio of $\delta E/\delta B$ (where δE is the amplitude of the electric field fluctuations and δB is the amplitude magnetic field fluctuation) to the theoretical dispersion relation indicates that the wave vector is oblique to the total magnetic field direction and that the observed component of the electric field has a large component along the k vector. This means that the wave is partly electrostatic and that the $\delta E/\delta B$ ratio does not indicate the phase velocity. We note that the wave frequency, as observed in the spacecraft frame, is less than the hydrogen gyrofrequency. The possibility that the observed wave frequencies are significantly Doppler-shifted from the value in the rest frame of the plasma is discussed in section 4. We confine much of the detailed analysis of this paper to below the ~ 4 Hz Nyquist frequency of the magnetic field data. However, it should be noted that the electric field data suggest that the duration of some of the spikes is as short as and perhaps shorter than the 10-Hz Nyquist frequency of the electric field data.

[18] An important feature of the small-scale waves illustrated in the top panel of Figure 2 is that they have an electric field amplitude that is similar to the amplitude of the large-scale Alfvén wave and a polarity in the same direction as the polarity of the large-scale Alfvén wave electric field. The magnetic field data behave differently. The magnetic field perturbations for the small-scale kinetic Alfvén waves are significantly smaller than the magnetic field perturbations associated with the larger-scale Alfvén wave. The fact that the electric field perturbations for large and small structures

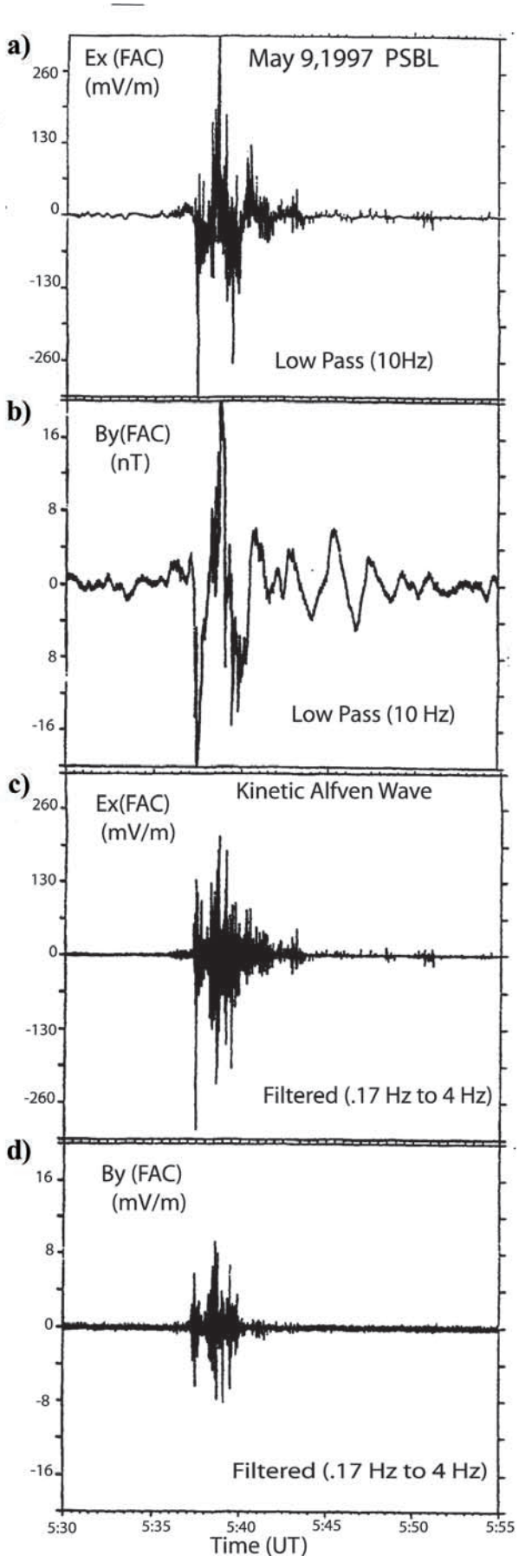

Figure 3. (opposite) (a, b) Polar measurements of the *Ex* component of the electric field at a time resolution of 10 Hz. (c, d) Detrended *Ex* and *By* components of the electric field filtered pass frequencies between 1 and 4 Hz.

are similar in amplitude indicates that the $\delta E \times B_0$ velocity variations induced by the large-scale Alfvén wave are similar in magnitude to those of the small-scale waves. In both cases the amplitude of the velocity variations is 200–500 km s^{-1} in a direction perpendicular to the average magnetic field and in the average plane of the plasma sheet. So any mechanisms explaining the relation (or absence of a relation) between the large-and small-scale structures ought to be able to explain why the wave electric field amplitudes are similar. This issue of the causal relation between the large-and small-scale electric fields will be addressed further in section 6.

[19] The bottom plot of Figure 2 shows that the Poynting flux parallel to the magnetic field associated with the kinetic Alfvén waves is ~25% of that of the large-scale Alfvén waves. It also shows that the Poynting flux is directed both parallel and antiparallel to the background magnetic field direction, implying no net transfer of electromagnetic energy up or down the magnetic field line due to these small-scale waves for this particular event. A more complete survey of the Poynting flux due to small-scale Alfvén waves using the Polar data set is planned. The existence of "small-scale" Poynting flux flowing both up and down the magnetic field line also indicates that the phase relation between the electric and magnetic field components of the small-scale waves is variable.

4. Scale Sizes and Perpendicular and Parallel Potential Drops

[20] Figure 4 presents the results of a theoretical calculation of the ratio of the component of the wave electric field perpendicular to the background magnetic field to the orthogonal component of the wave magnetic field also perpendicular to B. This figure is a modified version of a figure from *Lysak* [1998], based on a solution of the coupled Maxwell-Vlasov equations from *Lysak and Lotko* [1996]. We use Figure 4 to determine $k_\perp c/\omega_{Pe}$, where $k_\perp$ is the perpendicular wave number, c/ω_{Pe} ~10 km is the electron inertial length, c is the speed of light, and ω_{Pe} is the electron plasma frequency. The calculation of the linear dispersion relation includes full ion and electron gyroradius effects and electron kinetic effects in the regime where the wave frequency is less than the hydrogen gyrofrequency, $\beta \ll 1$, and $\beta \ll (k_\perp \rho_I)^2$. In our case the particle and magnetic field data indicate that β is fluctuating but on the order of 0.001. This analysis neglects nonlinear effects associated with electron convective derivatives that produce nonlinear steepening and that should be addressed in later and more sophisticated analyses. The dispersion relation assumes that the medium is both uniform and infinite in spatial extent. In reality, parallel gradients in the magnetic field magnitude and density variations may influence the properties of waves with sufficiently long parallel wavelengths. We neglect these effects in this preliminary and qualitative analysis. The dispersion relation assumes 100% H^+. The vertical scale is V_e^2/V_A^2, where V_A is the Alfvén velocity and V_e is the electron thermal velocity. A table describing

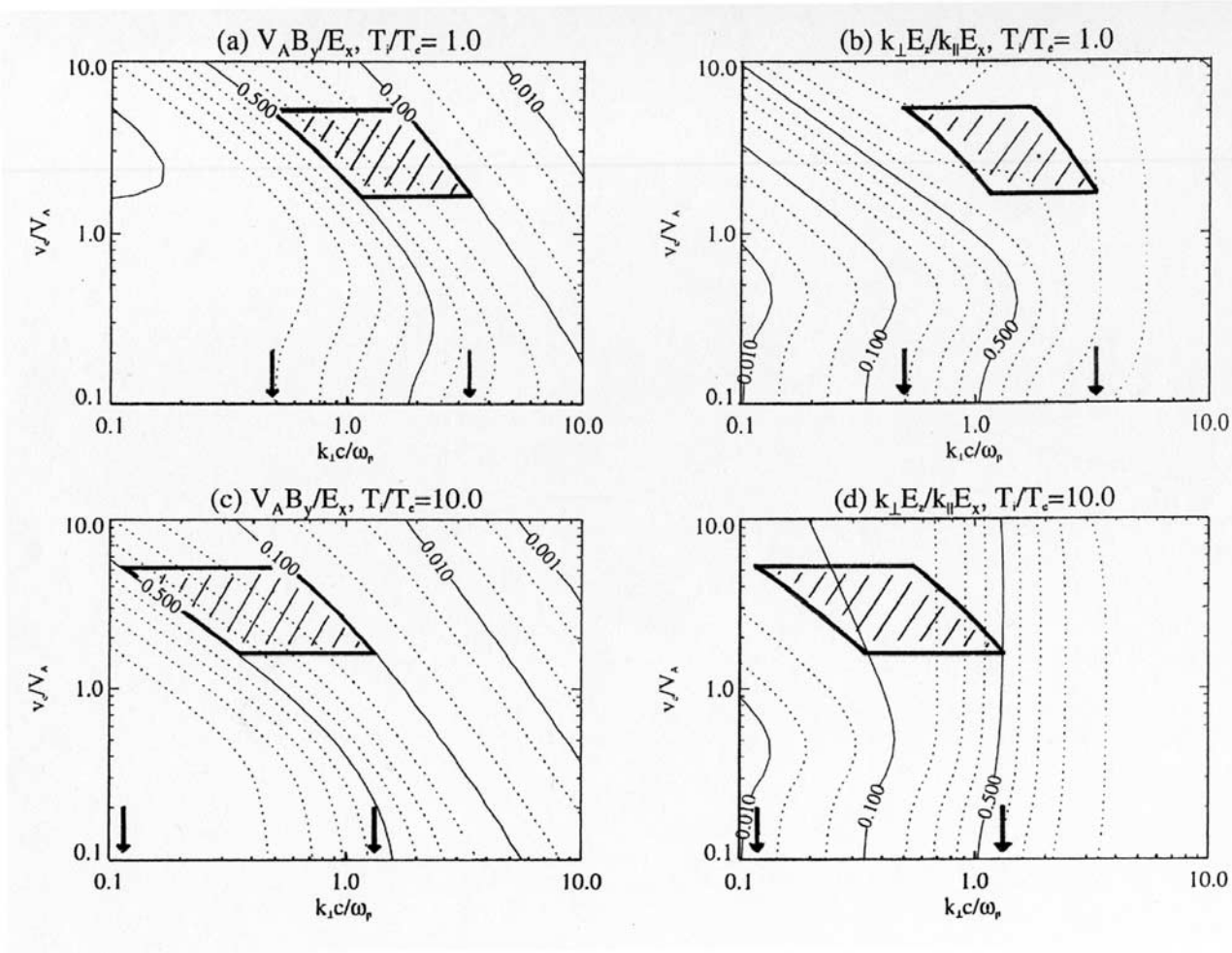

Figure 4. (a, c) Contours of theoretically calculated ($\delta B_Y/\delta E_X$) V_A for different values of V_e/V_A (vertical scale) and $k_\perp\rho$ (horizontal scale). The cross-hatched region delineates the experimentally derived values of ($|\delta B_y|/|\delta E_z|$) V_A (from data in Figure 2) for the experimental V_e/V_A. The horizontal range of the crosshatched region provides an estimate of $k_\perp\rho$=1−3. (b, d) Contours of theoretically calculated $k_\perp E_\parallel/k_\parallel E_\perp$ also versus V_e/V_A and $k_\perp\rho$. Using the experimentally determined V_e/V_A and the estimates of $k_\perp\rho$=1−3 from Figures 4b and 4d places the limits on $k_\perp E_\parallel/k_\parallel E_\perp$ illustrated by the crosshatched region.

the characteristic ion and electron temperatures, the electron inertial length, density, and ion gyroradius may be found in the work of *Wygant et al.* [2000]. In the case where the electrons and ions are anisotropic relative to the background magnetic field, the parallel electron temperature ∼2 keV is used to calculate the electron thermal velocity. An ion temperature perpendicular to B of 4 keV is used for T_i. The horizontal scale is $k_\perp c/\omega_{Pe}$. The contours delineate fixed values of the theoretical ratio of the amplitudes of the wave magnetic to the wave electric fields normalized to the Alfvén velocity. The ratios vary from those consistent with large-scale MHD waves on the extreme left-hand border of the plot to those more nearly electrostatic on the upper corner on the right-hand side of the lower panel. The superimposed, crosshatched parallelogram indicates the range of $\delta E/\delta B$ determined from different pulses in the data in Figures 3c and 3d and the experimentally determined values of V_e^2/V_A^2. As can be seen, this range of $\delta E_X/\delta B_Y$, observed for the ensemble of pulses, corresponds to $k_\perp c/\omega_{Pe}$ between 0.5 and 3 or $\lambda_\perp\sim$ 20−120 km for T_i/T_e = 1.

[21] Figures 4b and 4d provide information on the ratio of $\delta\phi_\parallel/\delta\phi_\perp$. Here $\delta\phi_\parallel \sim \int E_\parallel dl$, where the path integral is taken along a contour in a direction parallel to the magnetic field, where dl is the infinitesimal spatial displacement and E is the electric field vector. Here $\delta\phi_\parallel \sim \lambda_\parallel E_\parallel$, where $\lambda_\parallel$ is the wavelength (or scale size) parallel to B. Similarly, $\delta\phi_\perp \sim \int \delta E_\perp dl \sim \lambda_\perp E_\perp$ along a similar contour perpendicular to the ambient magnetic field. In each case the line integral of the electric fields contains nonpotential contributions due to the electromagnetic nature of the waves. The waves become more electrostatic at larger $k_\perp c/\omega_{Pe}$, and therefore $\delta\phi_\parallel/\delta\phi_\perp$ becomes closer to 1 as expected for potential structures. Figures 4b and 4d have the same horizontal and vertical axes as Figures 4a and 4c, so we can construct the same crosshatched box. In Figures 4b and 4d the contours indicate values of $\delta\phi_\parallel/\delta\phi_\perp = k_\perp E_\parallel/k_\parallel E$. Thus, using the value of $k_\perp$ derived from Figures 4a and 4c, the range of values for $\delta\phi_\parallel/\delta\phi_\perp$ is on the order of 0.5 to 1. Using $\lambda_\perp = 2\pi/k_\perp \sim$ 20−80 km, for a pulse amplitude of $E_\perp \sim$100 mV m^{-1}, $\delta\phi_\perp \sim$2000−8000 V, and $\delta\phi_\parallel \sim$100−4000 V. As mentioned in the previous

paragraph, this analysis assumes a uniform homogeneous medium, and therefore the estimated value of $\delta\phi_{||}$ is uncertain if the parallel wavelength of the kinetic Alfvén wave is comparable to the scale sizes of the gradients in ambient magnetic field magnitude, density, and temperatures. The perpendicular scale sizes of the small-scale waves of 20–80 km at 4–6 R_E would map to produce auroral structures on the order of 2–8 km at 100-km altitude. The mapping to low altitude of these structures is complicated by the fact that the structures with this scale size have a significant group velocity perpendicular to the magnetic field, resulting in a widening of the structure relative to a simple magnetic field line mapping.

[22] It is important to realize that this type of electric field structure with amplitudes of several hundred mV m^{-1} is observed routinely at high altitudes in the plasma sheet in the Polar data set with pulse durations as short as the time resolution of the 40 sample s^{-1} measurement nominal telemetry. The sampling rate of the Polar electric field through high time resolution bursts is ~8000 samples s^{-1}. At this data rate, the electric field spikes have been observed to have amplitudes up to several hundred mV m^{-1} with pulse durations ranging down to 10 ms. Since the fluxgate magnetic field measurements are strongly filtered at ~4 Hz to prevent aliasing, we cannot determine if the Alfvén waves with durations of <1/4 s have electric to magnetic field ratios characteristic of kinetic Alfvén waves. However, if they do, the observed amplitude of electric field pulses could provide parallel acceleration at perpendicular scales down to <5 km at 4–6 R_E. These structures could map to auroral features with perpendicular scales on the order of 400 m at 100-km altitude.

[23] The observed 1–4 Hz frequency of the small-scale waves in the spacecraft frame could be the consequence of a strong Doppler shift associated with the expansion of the plasma sheet and of their small perpendicular scale of the waves. A plasma sheet expansion velocity of V~40 km s^{-1} along with the estimated perpendicular scale size L~ 20 km s^{-1} would account for a Doppler shift of V/L ~ 2 Hz. This expansion velocity is reasonable but somewhat larger than the range of expansion velocities of 4–20 km s^{-1} estimated on the basis of very indirect arguments by *Wygant et al.* [2000]. Under these circumstances, the rest frame frequency of the small-scale waves would be much lower than the observed frequency in the spacecraft frame and could match the rest frame frequency of the large-scale waves. This would be consistent with the frequency matching condition necessary if the small-scale waves couple to the large-scale waves either through reflection off density perturbations or through some nonlinear interaction.

5. Parallel Electron and Ion Energization

[24] Figures 5a and 5b show a sequence of ion and electron 2-D velocity space distribution functions from the Hydra instrument during the period of the intense kinetic Alfvén wave spikes. Figures 5c–5e correspond to an expanded view of the electric and magnetic fields in Figure 3. Figure 5f is the negative of the spacecraft density, which provides information on the plasma electron thermal flux. Each distribution function is accumulated over 13 s, which is long compared to the duration of a single small-scale spike and comparable to the duration in the spacecraft frame of the large-scale Alfvén wave. Thus the observed distributions undoubtedly reflect the superposed effects of encounters with numerous wave structures. The horizontal axis is aligned along the magnetic field direction with the right-hand side corresponding to velocities toward the Earth. The distributions are reflected about the horizontal axis, so they are constrained to be symmetric about this axis. The electron distribution plots have a maximum velocity of 40,000 km s^{-1}, corresponding to an energy of ~4.44 keV. The maximum ion velocity is 1400 km s^{-1}, corresponding to an energy of ~10 keV.

[25] The first electron distribution function of the sequence is obtained within the low-density tail lobe and shows the characteristic isotropic distribution with a thermal energy <100 eV, low compared to the plasma sheet. Subsequent distributions are obtained in the outer boundary of the plasma sheet and show that the distributions have been energized in both the parallel and perpendicular directions with the parallel energies particularly enhanced. A clear example of an earthward electron beam feature is present in the second panel from the left in the bottom row of electron distributions (Figure 5b). An expanded view of this beam is presented in Figure 6. This electron beam feature coincides with the maximum in the electron energy flux at 0.7 ergs cm^{-2} s^{-1} in Figure 1d. Since the pitch angles of the electrons in the beam relative to the magnetic field direction are less than 20°, most of the electrons in the beam mirror are at altitudes less than 1.5 R_E. This means that a large portion of the beam can propagate to the auroral acceleration region. Thus one effect of the kinetic Alfvén waves observed at high altitude, in addition to their ability to energize the electrons, is to enhance the number of electrons that have access to the low-altitude acceleration region. These electrons could then be energized by any additional parallel electric field at lower altitudes. Another example of strong parallel energization occurs in the fourth panel from the left in the lower row of electron distributions (Figure 5b). In this case the electrons appear to be energized both parallel and antiparallel to the magnetic field. These features have a characteristic parallel energy on the order of ~1–2 keV. The perpendicular energy is 25–50 eV. The fact that the intense field-aligned electrons and particularly the earthward beam coincide with intense small-scale kinetic Alfvén wave structures that are theoretically predicted to have parallel electric potential drops on the order of 1 keV, suggests that the kinetic Alfvén waves could cause the observed energization parallel to the magnetic field.

[26] The ion distributions obtained during this time interval show beam-like ions flowing along the magnetic field away from the Earth with characteristic parallel energies on the order of 1–2 keV. These features are clearest in the second and third distributions of the top row of the ion distributions (Figure 5a) and in the third and fourth distributions of the bottom row. An expanded view of one of these ion beams is shown in Figure 6c. In principle, these ions could be energized by local parallel electric fields, by parallel electric fields at low altitudes in the auroral acceleration region, or by transverse acceleration mechanisms at low altitudes. In the latter scenario the magnetic mirror force results in a field-aligned beam-like structure at high altitudes. Within the context of the observations from Polar spacecraft, the ion acceleration at low altitudes could be

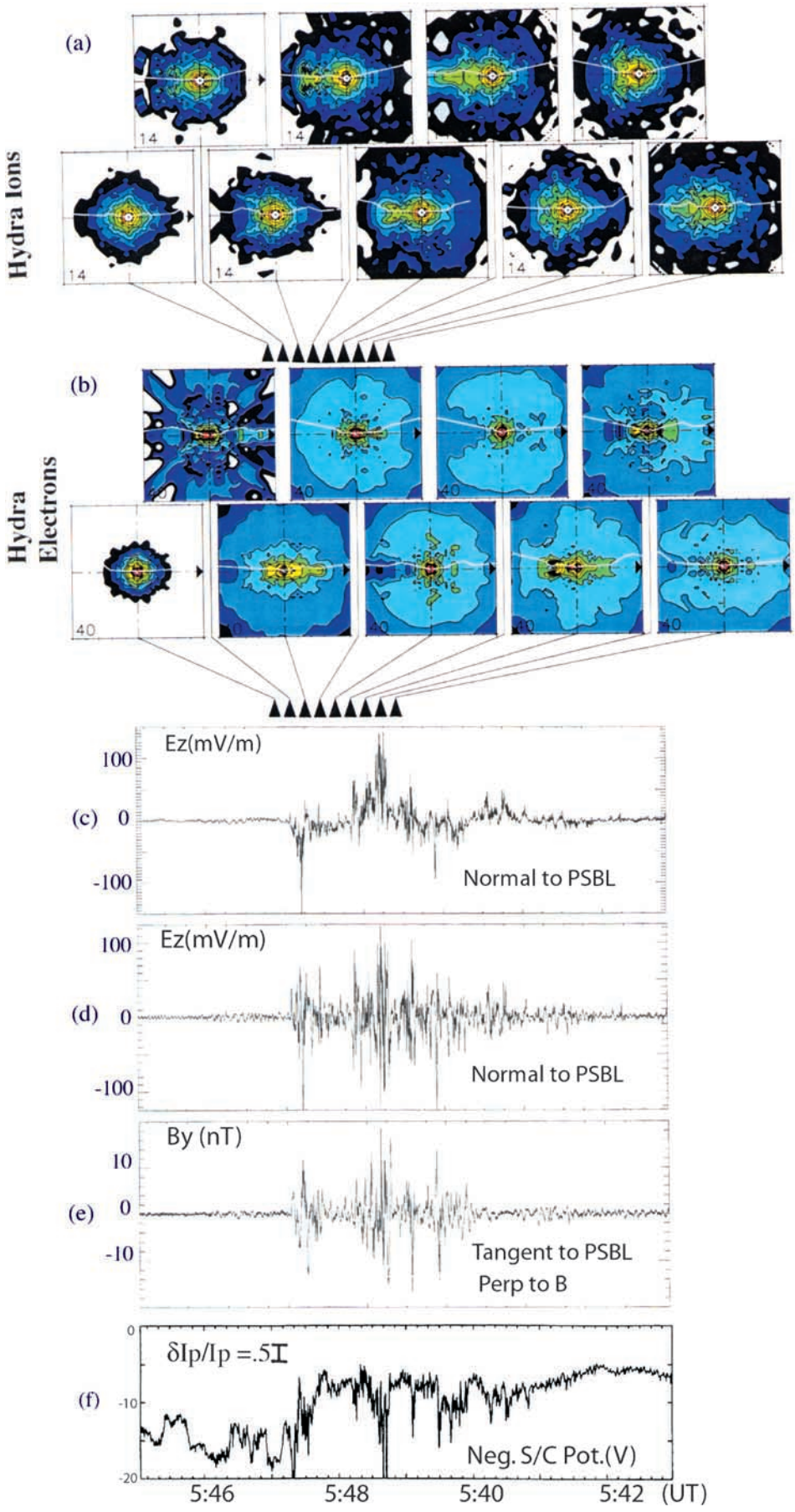
(a)
Hydra Ions
14
(b)
Hydra Electrons
40
(c)
Ez(mV/m)
100
0
-100
Normal to PSBL
(d)
Ez(mV/m)
100
0
-100
Normal to PSBL
(e)
By (nT)
10
0
-10
Tangent to PSBL
Perp to B
(f)
δIp/Ip =.5
0
-10
-20
Neg. S/C Pot.(V)
5:46
5:48
5:40
5:42
(UT)

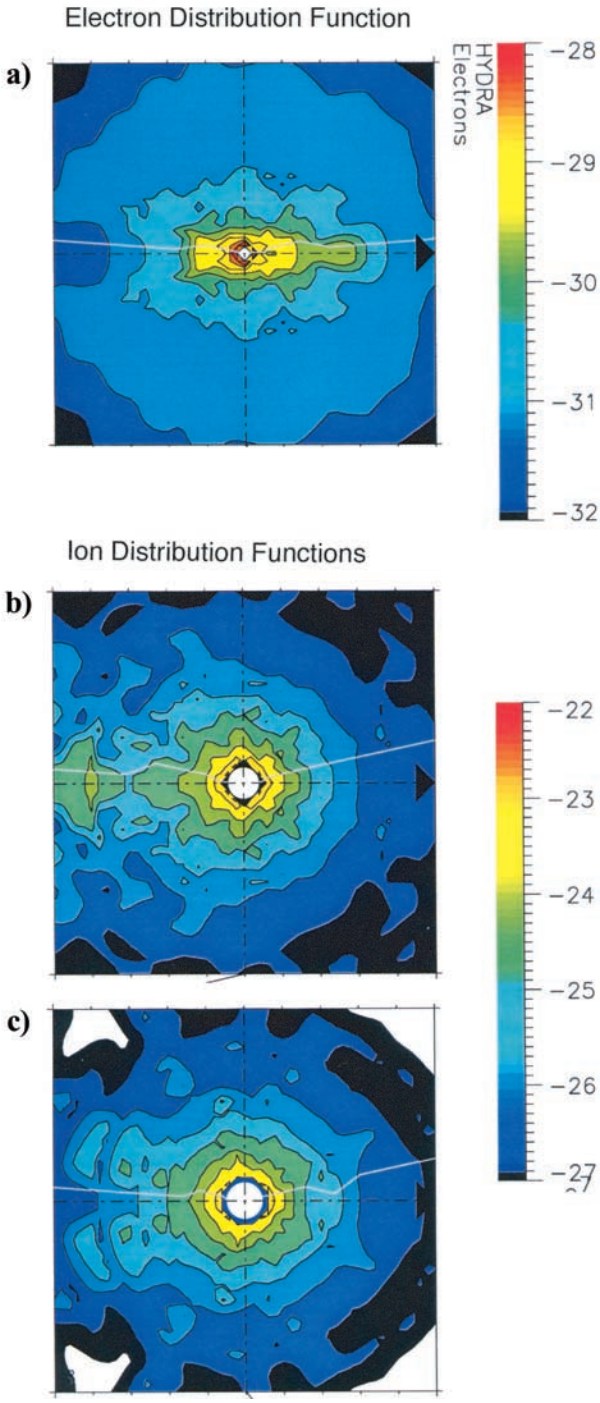

Figure 6. Expanded view from Figure 5 during a period of kinetic Alfvén waves of (a) an electron distribution function showing a beam-like structure and (b, c) ion distribution functions showing an ion conic and an upgoing ion beam, respectively.

powered by the locally observed Poynting flux as it propagates to lower altitudes, or the ions could be accelerated by the local parallel electric field associated with kinetic Alfvén waves. Either scenario explains the coincidence of Alfvénic structures and the upward flowing ions.

[27] As Figures 1 and 5 together show, the upward flowing ions, the earthward flowing electrons, the Alfvén waves carrying strong Poynting flux, and the small-scale kinetic Alfvén waves all occur within the same 3-min interval. The upward flowing electrons extend over a longer period. These occur in concert with the other phenomena but also persist deeper into the plasma sheet for several minutes. The above set of observations suggests that the most straightforward scenario for the acceleration of the earthward flowing electrons involves direct local acceleration by the parallel electric fields of the kinetic Alfvén waves. However, there is also the possibility that the electrons are accelerated at more distant locations along the magnetic field line (for example, the reconnection region or the auroral acceleration region in the Southern Hemisphere).

[28] Figure 5f shows that coincident with the most intense kinetic Alfvén waves are strong fluctuations in the electron thermal flux. The jump in the average value of the spacecraft potential at 0537:20 UT corresponds to the boundary between the plasma sheet and tail lobe and coincides with the density jump in the Hydra data. In this plasma regime a 2.5-V change in spacecraft potential corresponds to a ~50% fractional change in the electron thermal flux. In the hot (T_e ~ 0.1–1 keV) plasma sheet the spacecraft potential variations may be the consequence of either changes in electron energy or changes in electron density. This is unlike the situation presented by *Johnson et al.* [2001] in which the focusing effect on electron trajectories in Langmuir probe theory results in the spacecraft potential depending almost exclusively on density. Figure 5f shows that on timescales ranging down to the 1/2 s sampling rate for this quantity, there are 10–100% fluctuations in density and/or temperature of the plasma in the vicinity of the kinetic Alfvén waves at the PSBL.

6. Discussion

[29] In this paper we show for the first time that the large-scale Alfvénic fluctuations observed at and within the plasma sheet boundary layer, which carry large amounts of Poynting flux, are often intensely striated into numerous smaller-scale intense electric field spikes. We also provide the first evidence that small-scale spiky electric fields are kinetic Alfvén waves on the basis of their large ratio of the observed electric to magnetic field fluctuations. The analysis indicates that the measured waves should have appreciable values of $\delta\phi_{\parallel}$ on the order of 0.1 to several kV and should be efficient accelerators of electrons along the

Figure 5. (opposite) (a, b) Hydra electron and ion two-dimensional velocity space distribution functions parallel and perpendicular to the magnetic field obtained during a period of intense kinetic Alfvén waves from the 9 May 1997 plasma sheet crossing. The maximum electron velocities displayed are 40,000 km s^{-1}. The maximum ion velocity displayed is 1400 km s^{-1}. Velocities toward the Earth along the magnetic field line are along the horizontal axis to the right. (c) *Ez* at full 10-Hz resolution. (d, e) *Ez* and *By* filtered between 1/6 and 4 Hz. (f) Negative of the spacecraft potential, which is a measure of the plasma electron thermal flux (see text).

magnetic field. Direct measurement of velocity space distributions provides evidence for the parallel acceleration of electrons to energies of 0.1 to several keV. The most straightforward explanation of the parallel energization in the electron distribution functions is that the electrons are accelerated locally, but other scenarios are possible.

[30] The rigorous determination with a single spacecraft of the perpendicular spatial scale of the observed waves is difficult since the plasma sheet is known to expand and thin rapidly with unknown velocities. These plasma sheet velocities may be comparable to or larger than the typical velocity of the spacecraft, confounding attempts to determine scale sizes. Here a different approach is used. An examination of the experimental data indicates that the ratio of the electric field to magnetic field perturbations associated with the small-scale structures is $\delta E/\delta B \sim 2-5\ V_A$ instead of $\sim 1\ V_A$, as expected from MHD calculations and as measured for the simultaneously observed large-scale Alfvén wave. We compared the observed values of $\delta E/\delta B$ for the short time duration structures to theoretical calculations of this ratio by *Lysak* [1998] for kinetic Alfvén waves including both inertial and kinetic effects. This comparison was used to show that the observed range of $\delta E/\delta B$ for the small-scale structures is consistent with their identification as kinetic Alfvén waves with spatial scale sizes ranging below the ion gyroradius ($\sim$20 km) and the electron inertial length ($\sim$10 km). The estimates of the perpendicular scale size and the magnitude of the electric field ($\sim$100 mV m^{-1}) are used to show that the electric potential drops associated with individual spikes in directions perpendicular to the magnetic field are on the order of 100–5000 V. These values are comparable to the perpendicular potential variations seen at lower altitudes in large-amplitude electric structures first seen by the S3-3 spacecraft [*Mozer et al.*, 1977], which subsequent work has shown are responsible for auroral particle acceleration.

[31] *Hasegawa* [1976] first suggested that small-scale kinetic Alfvén waves possessed parallel electric fields and could be an efficient mechanism for accelerating particles on plasma sheet field lines. The kinetic Alfvén waves Hasegawa discussed had spatial scales perpendicular to B such that $k_\perp \rho_s \sim 1$, where ρ_s is the ion acoustic gyroradius. This is the "kinetic" limit of kinetic Alfvén waves. Subsequent theoretical investigations [*Goertz and Boswell*, 1979] focused on kinetic Alfvén waves in the electron inertial limit ($k_\perp c/\omega_{pe} \sim 1$) as a mechanism for establishing parallel electric fields capable of accelerating auroral electrons. Considerable experimental evidence has accumulated from the Viking, Freja, and FAST spacecraft, as well as low-altitude sounding rockets, that kinetic Alfvén waves in the inertial limit are an important feature of the altitude range between 1000 km and 2.5 R_E. *Lysak* [1998] and *Lysak and Lotko* [1996] have presented a model calculation of the properties of kinetic Alfvén waves along a magnetic flux tube in which the altitude range encompasses both regimes. The regime discussed in this paper is at an altitude range (4–7 R_E) in the plasma sheet in which both inertial and kinetic effects are important. There have not been reports of kinetic Alfvén waves in the plasma sheet itself or in any part of the magnetosphere above several R_E altitude. The observations presented herein provide evidence that intense kinetic Alfvén waves can play an important role in the creation of field-aligned electron distribution functions and in the parallel heating of electrons.

[32] The direct experimental detection of the parallel electric field component is difficult since it may be small (< 1 mV m^{-1}) compared to the perpendicular component ($\sim$100 mV m^{-1}) and extend over large distances parallel to the magnetic field. Alternatively, it may spontaneously organize into spatially localized structures and be encountered only occasionally. The theoretical calculations using the linear dispersion relation allowed an estimate of the value of $\int Edl$ along a direction parallel to the magnetic field for kinetic Alfvén wave structures of different scale sizes and ratios of v_A^2 / v_e^2 and T_e/T_i. These estimates of the parallel $\int Edl$ are $\sim$0.1 to 0.5 times the perpendicular $\int Edl$, ranging up to 3.5 keV for the 9 May 1997 event. A more complete analysis of the parallel electric field structure should account for the possibility that the parallel wavelength may be comparable or larger than the scale sizes of the parallel gradients in the Alfvén velocity as well as the electron inertial length and ion acoustic gyroradius. Future work could use nonlocal numerical codes similar to those presented by *Thompson and Lysak* [1996] or *Streltsov and Lotko* [1995].

[33] The electron distribution functions that coincide with these strong small-scale waves show strong evidence for parallel energization. In addition, a calculation of the energy flux of the electrons shows that there is a net flow of 0.7 ergs cm^{-2} s^{-1} earthward along the magnetic field in conjunction with the Alfvénic structures. The particle data also indicate local and parallel perpendicular energization of the ions.

[34] Several points can be made about the process of electron acceleration by the observed kinetic Alfvén waves and possible nonlinear effects involved in this turbulent nonlinear system. Since the waves propagate along the field line at about the Alfvén velocity ($\sim$10,000 km s^{-1}), and this velocity is comparable to a typical parallel thermal velocity for a several hundred eV electron, a large fraction of the electron distribution function may interact strongly with the wave. This interaction may consist of both Fermi reflection off the advancing wave front in one or more encounters and/or trapping in the variations of the parallel fluctuations of $\delta\phi_\parallel$. These processes of electron trapping and reflection could produce significant effects on the electron distribution function since $\delta\phi_\parallel$ also ranges between 100 V and several kilovolts, producing a trapping width that is comparable to the thermal energy spread of the observed distribution functions. The reflection process results in the acceleration of a stationary electron up to velocities of $2V_A$ in the rest frame of the plasma as illustrated in the simulations of *Kletzing* [1994]. Trapping in wave troughs is important when the trapping frequency ω_T is comparable to or larger than ω, the frequency of the wave [*Davidson*, 1972]. The trapping frequency is given by $\omega_T = k_\parallel (e\delta\phi_\parallel/m_e)^{1/2} \sim 1-10$ Hz for parallel wavelengths of $\sim$1000–10,000 km. If the rest frame frequency of the kinetic Alfvén waves is roughly similar to the observed frequency in the spacecraft frame (1–10 Hz), then the trapping frequency is comparable to the rest frame frequency, and the trapping of electrons could be an important dynamic feature of this data set. *Hui and Seyler* [1992] have self-consistently simulated the effects of trapping on the spectrum of kinetic Alfvén waves in the

inertial limit for conditions appropriate to lower altitudes. Their hybrid simulation shows that the trapping can lead to the production of large-amplitude, smaller-scale kinetic Alfvén wave structures.

[35] The fact that $e\delta\phi_{\|}/T_e = 0.1-1$ suggests through the linearized Boltzmann relation [*Hasegawa and Mima*, 1978] that the observed kinetic Alfvén waves have a compressive component that can induce significant density fluctuations, $e\delta\phi_{\|}/T_e = \delta n_e/n_{e0} = 0.1-1$. Although the electron density is sampled by the Hydra instrument on 13-s timescales, the spacecraft potential at a sampling rate of 2 samples s^{-1} also responds to electron density and temperature fluctuations in this plasma regime. This quantity provides evidence during the period of kinetic Alfvén waves for 10–100% variations in the electron thermal flux from the plasma on timescales ranging down to the 2 sample s^{-1} resolution of the instrument. These variations in thermal flux could be due to either small temporal/spatial scale temperature or density variations. The variations in density and/or temperature provide an extremely nonuniform and irregular medium through which both large- and small-scale Alfvén waves must propagate.

[36] In section 1 we showed that the small-scale Alfvénic structures coincide with the observations of larger-scale Alfvén waves carrying a significant Poynting flux. Furthermore, both the amplitude and direction of the electric field associated with the small-scale spikes are similar to that of the large-scale Alfvén wave. Since the large-scale waves carry more Poynting flux than do the small-scale waves, we argue on the basis of energetics that the large-scale waves generate the smaller-scale waves. A variety of models can be invoked to explain the coupling between the large-scale Alfvén waves and the smaller-scale kinetic Alfvén wave structures. *Hasegawa* [1976] was the first to suggest that Alfvénic surface waves could couple to kinetic Alfvén waves via an interaction with the density gradient at the plasma sheet–tail lobe boundary. In addition, it is possible that small-scale density variations interact with either the large-scale Alfvén wave or other small-scale kinetic Alfvén waves propagating through the medium. Such interactions with density gradients could result in the further production of small perpendicular scale size structures through processes that invoke reflection and refraction of incident wave fronts off the variations in the index of refraction [*Lysak and Song*, 2000].

[37] Alternatively, the $E \times B$ velocity induced by a large-scale Alfvén wave could produce a velocity shear, which would drive the magnetized Kelvin-Helmholtz instability and produce small perpendicular-scale perturbations. This velocity shear as well as the tearing mode instability (driven by the free energy in the perturbation magnetic field of the large-scale Alfvén wave) has been investigated as a mechanism for generating kinetic Alfvén waves on auroral field lines in the inertial limit [*Seyler*, 1988]. As discussed, additional structure of waves can occur if electrons are trapped in the kinetic Alfvén waves [*Hui and Seyler*, 1992]. Density gradients perpendicular to the magnetic field can reflect and refract large-scale Alfvén waves and thereby produce small perpendicular-scale kinetic Alfvén waves. This mechanism has been discussed in the inertial limit by *Lysak and Song* [2000]. Finally, it is possible for kinetic Alfvén waves to be generated directly from the free energy in the density and temperature variations at the tail lobe–plasma sheet density jump [*Maggs et al.*, 1997]. In this scenario the small-scale waves would not necessarily be directly related to the large-scale Alfvén wave.

[38] The observations of these processes present some insight and raise questions about the global dynamics of the magnetosphere during magnetospheric substorms. *Keiling et al.* [2001] and *Toivanen et al.* [2001] provide evidence that intervals of strong Poynting flux at the PSBL are associated with the onsets and/or expansion phases of substorms. The relatively brief duration of the Poynting flux bursts as observed in the spacecraft frame (1–3 min) in comparison to the duration of substorm expansion phases can be explained by the fact that during the expansion phase of the substorm the plasma sheet expands rapidly over the spacecraft carrying with it the PSBL and its associated Poynting flux layer. For this reason, the perpendicular spatial extent of the Poynting flux and small-scale kinetic Alfvén waves flowing on auroral/PSBL field lines is not known. Comparison to Ultraviolet Imager (UVI) images of the aurora and the associated inferred energy flux in auroral electron beams presented by W1 suggests that the region of strong Poynting flux may supply the energy to structures 1°–2° in latitudinal extent. This implies that the width of the layer of Poynting flux at 4–7 R_E in the PSBL is 1000–3000 km. In this scenario, Poynting flux along the PSBL is one (if not the) major energy transfer mechanism during substorm energy release processes. The field-aligned electron distributions, which coincide with the kinetic Alfvén waves, carry an energy flux toward the Earth on the order of 0.5 ergs cm^{-2} s^{-1}. The Poynting flux associated with the large-scale Alfvén waves is on the order of 1.25 ergs cm^{-2} s^{-1} over 6-s averages. If evaluated on timescales of 0.5 s, the peak value of the Poynting flux is on the order of 4 ergs cm^{-2} s^{-1}. The data presented here show that the Poynting flux associated with the large-scale Alfvén waves dominates over the Poynting flux associated with the large-scale convection electric field and the magnetic field perturbation associated with the large-scale field-aligned current systems by orders of magnitude.

[39] Since the electric fields associated with the Alfvén waves are oriented primarily normal to the plasma sheet boundary and no spacecraft with booms oriented in this direction has explored the outer boundary of the plasma sheet at higher altitudes, the high-altitude extent of the large- and small-scale Alfvén waves is not known. Thus, in principle, the waves could extend all the way to the reconnection region and involve heating and acceleration all along the outer boundary of the plasma sheet. These waves may be one of the principal mechanisms for heating particles throughout the plasma sheet to keV energies.

[40] The existence of a large-energy flux along the outer boundary of the plasma sheet suggests that these field lines map to a more distant region, which is a significant energy source. Since the outer boundary of the plasma sheet delineates the boundary between open and closed field lines, it is tempting to presume that this energy source is the reconnection region and that an appreciable portion of the energy released in the reconnection region is radiated toward the Earth along magnetic field lines as Alfvén waves. If so, an important experimental question is whether the Poynting flux observed at the outer boundary of the

plasma sheet is generated directly by the reconnection region, or whether the Poynting flux is derived from ion beams that are accelerated away from the reconnection region and that are unstable to Alfvén waves.

[41] The acceleration of charged particles by kinetic Alfvén waves has several properties that are of special interest within the general context of space and astrophysical particle acceleration. The acceleration of electrons by small-scale kinetic Alfvén waves involves the creation of parallel electric fields that can appear as a consequence of the linear properties of the waves (which include either electron dispersion and/or finite ion gyroradius effects). The effects and the waves can be present anywhere within a very large volume of space in a nearly uniform, low-density, collisionless magnetized plasma. This is in contrast to many of the mechanisms responsible for the acceleration of auroral electrons beams at lower altitudes that rely on a variety of effects occurring only in the strongly converging magnetic field configurations near the Earth or other planets. For example, altitudes of $1-2\ R_E$ in the auroral acceleration region of the Earth are understood to be important for parallel acceleration on the basis of theoretical arguments that discuss the limited current-carrying capacity of the plasma in density cavities in converging magnetic field configurations. Plasma sheath phenomena producing parallel electric fields, magnetic mirror forces, and the low thresholds for current-driven instabilities are all most likely to be strongest at lower altitudes. The scenario presented here, the generation of large-amplitude Alfvén waves, their striation or filamentation into small-scale kinetic Alfvén wave structures, and the subsequent acceleration of electrons due to the associated parallel electric field, is a process that can occur over very large volumes of space in comparatively uniform and weak magnetic field regions. The other major energization mechanisms operating far from the planet surface or astrophysical body are commonly associated with compressional fast mode shock waves. Fast mode shocks are much more commonly invoked than is kinetic Alfvén wave acceleration for a variety of space and astrophysical scenarios. However, it has become increasingly clear [*Holleweg*, 1999, and references therein] that there are important space and astrophysical scenarios in which kinetic Alfvén waves provide a potentially important competitive and efficient energization mechanism. It appears that this class of acceleration mechanisms may be especially important when the nature of the free energy sources in the system drive large-scale MHD Alfvén waves and when coupling to small-scale structures occurs.

[42] It is clear that the interaction between the wave fields and particle populations at the PSBL is sufficiently complicated that our ideas on the important dynamics will evolve as they are subjected to the constraints of a larger data set of plasma sheet crossings, the availability of higher time resolution data from this and other spacecraft, more rigorous analysis of spatial scales from appropriately instrumented multispacecraft missions, and more sophisticated theoretical analysis than presented here.

[43] **Acknowledgments.** Analysis of electric field data at the University of Minnesota was supported by NASA International Solar Terrestrial Program (NASA contract NAG 5-3182). Theoretical work at the University of Minnesota was supported by a UMN subcontract from UCB SA1470-23290PG on NASA grant NAG 5 8082. Analysis of magnetometer data was supported by NASA ISTP grant 5-3217. Work at the University of Iowa in analysis of Hydra data was performed under NASA grant NAG 5 2231 and DARA grant 50 OC 8911 0. The results of the Hydra investigation were made possible by the decade-long hardware efforts of groups led at NASA GSFC by K. Ogilvie, at UNH by R. Torbert, at MPAe by A. Korth, and at UCSD by W. Fillius. We would also like to thank Reiner Friedel and coworkers for use of the PAPCO graphical display program.

[44] Hiroshi Matsumoto thanks J. R. Johnson and another referee for their assistance in evaluating this paper.

References

Block, L. P., and C.-G. Falthammer, The role of magnetic-field-aligned electric fields in auroral acceleration, *J. Geophys. Res.*, *95*, 5877, 1990.

Carlson, C. W., R. F. Pfaff, and J. G. Watzin, The Fast Auroral Snapshot (FAST) mission, *Geophys. Res. Lett.*, *25*, 2013, 1998.

Cattell, C. A., M. Kim, R. P. Lin, and F. Mozer, Observations of large electric fields at the plasma sheet boundary layer by ISEE-1, *Geophys. Res. Lett.*, *9*, 539, 1982.

Davidson, R. C., *Methods in Nonlinear Plasma Theory*, Academic, San Diego, Calif., 1972.

Eastman, T. E., L. A. Frank, W. K. Peterson, and W. Lennartsson, The plasma sheet boundary layer, *J. Geophys. Res.*, *89*, 1553, 1984.

Ergun, R. E., et al., Fast satellite observations of electric field structures in the auroral zone, *Geophys. Res. Lett.*, *25*, 2025, 1998.

Fairfield, D. H., Structure of the geomagnetic tail, in *Magnetotail Physics*, edited by A. T. Lui, p. 23, John Hopkins Univ. Press, Baltimore, Md., 1987.

Goertz, C. K., Kinetic Alfven waves on auroral field lines, *Planet. Space Sci.*, *32*, 1503, 1984.

Goertz, C. K., and R. W. Boswell, Magnetosphere-ionosphere coupling, *J. Geophys. Res.*, *84*, 7239, 1979.

Harvey, P., et al., The Electric Field Instrument on the Polar satellite, *Space Sci. Rev.*, *71*, N1-4, 1995. (Reproduced in *The Global Geospace Mission,* edited by C. T. Russell, p. 583, Kluwer Acad., Norwell, Mass., 1995.)

Hasegawa, A., Particle acceleration by MHD surface wave and formation of the aurora, *J. Geophys. Res.*, *81*, 5083, 1976.

Hasegawa, A., and L. Chen, Kinetic process of plasma heating due to Alfvén wave excitation, *Phys. Res. Lett.*, *35*, 370, 1975.

Hasegawa, A., and K. Mima, Anomalous transport produced by kinetic Alfven wave turbulence, *J. Geophys. Res.*, *83*, 1117, 1978.

Holleweg, J. V., Kinetic Alfvén wave revisited, *J. Geophys. Res.*, *104*, 14,811, 1999.

Hui, C.-H., and C. E. Seyler, Electron acceleration by Alfvén wave in the magnetosphere, *J. Geophys. Res.*, *97*, 3953, 1992.

Keiling, A., J. R. Wygant, C. Cattell, M. Johnson, M. Temerin, F. Mozer, C. A. Kletzing, J. Scudder, C. T. Russell, and W. Peterson, Properties of large electric fields in the plasma sheet at $4-7\ R_E$ measured with Polar, *J. Geophys. Res.*, *106*, 5779, 2001.

Kletzing, C. A., Electron energization by kinetic Alfvén waves, *J. Geophys.Res.*, *99*, 11,095, 1994.

Johnson, M., J. R. Wygant, C. Cattell, F. S. Mozer, M. Temerin, and J. Scudder, Observations of the seasonal dependence of the thermal plasma density in the Southern Hemisphere auroral zone and polar cap at 1 R_E, *J. Geophys. Res.*, *106*, 19,023, 2001.

Louarn, P., J. E. Wahlund, T. Chust, H. deFeraudy, A. Roux, B. Holback, P. O. Dovner, A. I. Eriksson, and G. Holmgren, Observation of kinetic Alfvén waves by the FREJA spacecraft, *Geophys. Res. Lett.*, *21*, 1847, 1994.

Lysak, R. L., The relationship between electrostatic shocks and kinetic Alfvén waves, *Geophys. Res. Lett.*, *25*, 2089, 1998.

Lysak, R. L., and W. Lotko, On the dispersion relation for shear Alfvén waves, *J. Geophys. Res.*, *101*, 5085, 1996.

Lysak, R. L., and Y. Song, The role of Alfvén waves in the formation of the auroral parallel electric fields, in *Magnetospheric Current Systems*, *Geophys. Monogr. Ser.*, vol. 118, edited by S. Ohtani et al., p. 147, AGU, Washington, D.C., 2000.

Maggs, J. E., G. J. Morales, and W. Gekelman, Laboratory studies of field-aligned density striations and their relationship to auroral processes, *Phys. Plasmas*, *4*(5), 1881, 1997.

Maynard, N. C., W. J. Burke, E. M. Basinska, G. M. Erickson, W. J. Hughes, H. J. Singer, A. G. Yahnin, D. A. Hardy, and F. S. Mozer, Dynamics of the inner magnetosphere near times of substorm onsets, *J. Geophys. Res.*, *101*, 7705, 1996.

Mozer, F. S., and A. Hull, Origins and geometry of upward parallel electric fields in the auroral acceleration region, *J. Geophys. Res.*, *106*, 5763, 2001.

Mozer, F. S., et al., Observation of paired electrostatic shocks in the polar magnetosphere, *Phys. Rev. Lett.*, *38*, 292, 1977.

Mozer, F. S., et al., Satellite measurements and theories of low-altitude auroral particle acceleration, *Space Sci. Rev.*, *27*, 155, 1980.

Mozer, F. S., et al., New features of time domain electric field structures in the auroral acceleration region, *Phys. Rev. Lett.*, *79*, 1281, 1997.

Pedersen, A., et al., Electric fields in the plasma sheet and plasma sheet boundary layer, *J. Geophys. Res.*, *90*, 1231, 1985.

Reiff, P. H., et al., On the high-and low-altitude limits of the auroral electric field region, in *Auroral Plasma Dynamics, Geophys. Monogr. Ser.*, vol. 80, edited by R. L. Lysak, p. 143, AGU, Washington, D.C., 1993.

Russell, C. T., R. C. Snare, J. D. Means, D. Pierce, D. Dearborn, M. Larson, G. Barr, and G. Le, The GGS/Polar Magnetic Fields Investigation, *Space Sci. Rev.*, *71*, N1-4, 1995. (Reproduced in *The Global Geospace Mission*, edited by C. T. Russell, Kluwer Acad., Norwell, Mass., 1995.)

Scudder, J., et al., Hydra: A 3-dimensional electron and ion hot plasma instrument for the Polar spacecraft of the GGS mission, in *The Global Geospace Mission*, edited by C. T. Russell, p. 495, Kluwer Acad., Norwell, Mass., 1995.

Seyler, C. E., Nonlinear 3-D evolution of bounded kinetic Alfvén waves due to shear flow and collisionless tearing instability, *Geophys. Res. Lett.*, *15*, 756, 1988.

Streed, T., C. Cattell, F. Mozer, S. Kokubun, and K. Tsuruda, Spiky electric fields in the magnetotail, *J. Geophys. Res.*, in press, 2002.

Streltsov, A. V., and W. Lotko, Dispersive field line resonances on auroral field lines, *J. Geophys. Res.*, *100*, 19,457, 1995.

Temerin, M., and I. Roth, Ion heating by waves with frequencies below the ion gyrofrequency, *Geophys. Res. Lett.*, *13*, 1109, 1986.

Temerin, M., et al., Production of flickering aurora and field-aligned electron flux by electromagnetic ion cyclotron waves, *J. Geophys. Res.*, *91*, 5769, 1986.

Thomson, B. J., and R. L. Lysak, Electron acceleration by inertial Alfven waves, *J. Geophys. Res.*, *101*, 5359, 1996.

Toivanen, P. K., D. N. Baker, W. K. Peterson, X. Li, E. F. Donovan, A. Viljanen, A. Keiling, J. R. Wygant, and C. A. Kletzing, Plasma sheet dynamics observed by the Polar spacecraft in association with substorm onsets, *J. Geophys. Res.*, *106*, 19,117, 2001.

Tsyganenko, N. A., A magnetospheric magnetic field model with a warped tail current sheet, *Planet. Space Sci.*, *37*, 5, 1989.

Weimer, D. R., and D. A. Gurnett, Large-amplitude auroral electric fields measured with DE 1, *J. Geophys. Res.*, *98*, 13,557, 1993.

Wygant, J. R., et al., Polar spacecraft based comparisons of intense electric fields and Poynting flux near and within the plasma sheet tail lobe boundary to UVI images: An energy source for the aurora, *J. Geophys. Res.*, *105*, 18,675, 2000.

C. A. Cattell, A. Keiling, R. L. Lysak, and J. R. Wygant, School of Physics and Astronomy, University of Minnesota, 116 Church St. S.E., Minneapolis, MN 55455, USA. (cattell@belka.space.umn.edu; akeiling@belka.space.umn.edu; bob@aurora.spa.umn.edu; wygant@belka.space.umn.edu)

C. A. Kletzing and J. D. Scudder, Department of Physics and Astronomy, University of Iowa, Iowa City, IA 52242, USA.

W. Lotko and V. Streltsov, Thayer School of Engineering, Dartmouth College, Hanover, NH 03755, USA.

F. S. Mozer and M. Temerin, Space Sciences Laboratory, University of California at Berkeley, Berkeley, CA 94720, USA.

C. T. Russell, IGPP, University of California, Los Angeles, CA 90024, USA. (ctrussell@igpp.ucla.edu)